ELSEVIER

Biochimica et Biophysica Acta 1571 (2002) 45–54

BIOCHIMICA ET BIOPHYSICA ACTA
BBA

www.bba-direct.com

Kinetics of phosphate-mediated oxidation of ferrous iron and formation of 8-oxo-2′-deoxyguanosine in solutions of free 2′-deoxyguanosine and calf thymus DNA

Peter Svoboda, Mats Harms-Ringdahl*

Department of Genetic and Cellular Toxicology, Arrhenius Laboratories for Natural Sciences, Stockholm University, Stockholm S-106 91, Sweden

Received 18 October 2001; received in revised form 21 February 2002; accepted 26 March 2002

Abstract

Formation of 7,8-dihydro-8-oxo-2′-deoxyguanosine (8-oxo-dG) in solutions of free 2′-deoxyguanosine (dG) and calf thymus DNA (DNA) was compared for the diffusion-dependent and localised production of oxygen radicals from phosphate-mediated oxidation of ferrous iron (Fe^{2+}) to ferric iron (Fe^{3+}). The oxidation of Fe^{2+} to Fe^{3+} was followed at 304 nm at pH 7.2 under aerobic conditions. Given that the concentration of $Fe^{2+} \geq$ phosphate concentration, the rate of Fe^{2+} oxidation was significantly higher in DNA-phosphate as compared for the same concentration of inorganic phosphate. Phosphate catalysed oxidation of ferrous ions in solutions of dG or DNA led through the production of reactive oxygen species to the formation of 8-oxo-dG. The yield of 8-oxo-dG in solutions of dG or DNA correlated positively with the inorganic-/DNA-phosphate concentrations as well as with the concentrations of ferrous ions added. The yield of 8-oxo-dG per unit oxidised Fe^{2+} were similar for dG and DNA; thus, it differed markedly from radiation-induced 8-oxo-dG, where the yield in DNA was several fold higher. For DNA in solution, the localisation of the phosphate ferrous iron complex relative to the target is an important factor for the yield of 8-oxo-dG. This was supported from the observation that the yield of 8-oxo-dG in solutions of dG was significantly increased over that in DNA only when Fe^{2+} was oxidised in a high excess of inorganic phosphate (50 mM) and from the lower protection of DNA damage by the radical scavenger (hydroxymethyl)aminomethane (Tris)–HCl.

Keywords: 8-oxo-dG; Fenton; DNA; 2′-Deoxyguanosine; Phosphate; Iron

1. Introduction

Oxidative DNA damage has been correlated to mutagenesis, carcinogenesis, several other diseases and the process of aging in general [1–6]. Oxidative damage is also found in proteins, membranes and in the intracellular pool of nucleotides [7,8]. Oxidative processes such as in the respiratory chain where low levels of superoxide ($O_2^{-\bullet}$) are formed, can lead to the formation of H_2O_2 and Fenton chemistry [9,10], producing reactive oxygen species such as hydroxyl radicals. Formation of 7,8-dihydro-8-oxo-2′-deoxyguanosine (8-oxo-dG) has been detected in nuclear DNA after exposure to reactive oxygen species derived from irradiation, metal catalysed systems or different chemical agents [1,11]. 8-Oxo-dG gives unspecific base pairing and also causes adjacent bases to loose their base pairing specificity [7,9]. This may lead to both mutagenesis and carcinogenesis [1,10]. Several repair functions [7,9,12,13] that remove 8-oxo-dG from DNA have been described, as well as enzymes that prevent modified nucleotides such as 8-oxo-dG triphosphate in the nucleotide pool to be incorporated into DNA [7]. The existence of these cellular defence mechanisms shows that the formation of oxidative damages in both DNA and the nucleotide pool of the cell has biological significance, and motivates further studies of the mechanism of radical production in different cellular compartments.

Transition metals such as iron and copper catalyse Fenton type of reactions under in vitro conditions but may also be involved in the endogenous processes of oxidation of biomolecules in oxygen-containing biological systems [14,15]. Ferrous ions are readily oxidised to ferric ions in response to complex formation with phosphate [14,16–19] as well as pyrophosphate, polyphosphate [20], DNA [21] or nucleotides in the di- or triphosphate form [22,23]. Several studies have shown that during the oxidation, superoxide ($O_2^{-\bullet}$) is

* Corresponding author. Tel.: +46-8-164109; fax: +46-8-164315.
E-mail address: mats.harms-ringdahl@genetics.su.se (M. Harms-Ringdahl).

0304-4165/02/$ - see front matter
PII: S0304-4165(02)00205-2

formed, leading to the subsequent production of H_2O_2 and Fenton type of reactions [10,17]. Thus, chelation of ferrous ions with DNA-phosphate would be expected to increase oxygen radical formation close to DNA and cause a broad spectrum of different types of DNA damage [21,24,25]. It is also possible that iron chelated to nucleotides in the cellular nucleotide pool could generate oxygen radicals forming modified nucleotides, which, if incorporated into newly synthesised DNA, could lead to mutations, as described above. Free radical-induced damage on DNA can be studied using several different markers such as strand breaks, base loss and base damages. The formation of 8-oxo-dG has been attributed to the attack of hydroxyl radicals [1,11], thus making it a suitable marker for Fenton chemistry.

The aim of this study was to compare the kinetics for the phosphate catalysed oxidation of ferrous iron in solutions of target localised phosphate (DNA-phosphate) or free phosphate (inorganic phosphate) and to analyse for differences regarding the formation of the base damage 8-oxo-dG in DNA or free 2′-deoxyguanosine (dG). We have previously observed that the yield of 8-oxo-dG in irradiated solutions of DNA was 20 fold higher as compared to solutions of dG [26]. Thus, a comparison of the effects of radiation-induced radical formation with Fenton chemistry on the yields of 8-oxo-dG could give further knowledge of the mechanisms for oxygen radical-induced damage to DNA and nucleotides under endogenous or radiation-exposed conditions.

2. Materials and methods

2.1. Chemicals

dG-monohydrate was obtained from Fluka (Switzerland). Calf thymus DNA, a highly polymerised DNA sodium salt containing 7.8% sodium and 10.3% water, was from Sigma (USA). The DNA was prepared in a Falcon tube filled with water and gently shaken overnight at 4 °C. Tris(hydroxymethyl)aminomethane (Tris) and maleic acid were also purchased from Sigma. $FeSO_4$ and $FeCl_3$ were from Merck (Germany). Stock solution of $FeSO_4$ was prepared in 5 mM H_2SO_4 (to prevent oxidation). Stock solution of $FeCl_3$ was prepared in water. Sodium phosphate was from Merck and sodium hydroxide from Eka Nobel (Sweden). 8-oxo-dG used for making standard solutions was from Sigma. Water used for washing of vials and preparing stock solutions was double-deionised ($R > 18$ MΩ-cm).

2.2. Enzymes

Nuclease P1 (*Penicillium citrinum*) from Amersham Pharmacia Biotech (Sweden) was dissolved in 100 mM Tris–HCl buffer (pH 7.2). Alkaline phosphatase (calf intestinal mucosa) from the same company was dissolved in 100 mM Tris–HCl buffer (pH 8.2). Catalase from bovine liver, a suspension in water containing 0.1% thymol was obtained from Sigma. Heat-inactivated catalase was prepared by heating the enzyme for 30 min at 80 °C.

2.3. Oxidation of Fe^{2+} to Fe^{3+}

Oxidation of 0.1 mM ferrous iron (Fe^{2+}) to ferric iron (Fe^{3+}) was followed at 304 nm in the presence of up to 1.0 mM inorganic phosphate or calf thymus DNA in quartz cuvettes under aerobic conditions, using a Shimadzu spectrophotometer. The oxidation was followed during a period of 13 min at 22 °C in a Tris–HCl buffer, 10 mM, to keep pH constant at 7.2. With the same optical method and concentrations, the pH dependence for oxidation of ferrous iron in the presence of inorganic phosphate or calf thymus DNA was followed in Tris–maleate buffer, 10 mM, at four different pH values, pH 6.8, 7.2, 7.6 and 8.1. We observed that the molar absorbance coefficient of ferric ions was dependent on the phosphate concentration and thus we experimentally determined the wavelength that was least affected of this dependency to be 304 nm, not far from the wavelength (300 nm) previously used by others [19,27]. The influence of phosphate on the molar absorbance coefficient was corrected for with the equations presented in Table 1. The equations represent the linear response for the absorbance dependency of ferric ions on the concentration of inorganic or DNA phosphate in Tris–HCl or Tris–maleate buffer (Table 1). Tris–HCl was chosen, due to its low effect on Fe^{2+} autoxidation in comparison with phosphate ions [14,18,28]. Also, Tris–HCl is an effective hydroxyl radical scavenger and the rate constant for reaction of hydroxyl radicals with Tris–HCl has been measured to be 1.1×10^9 M^{-1} s^{-1} [29].

2.4. Induction of 8-oxo-dG

To induce 8-oxo-dG formation, $FeSO_4$ (0.1 or 0.2 mM) was added to mixtures of dG or DNA in Eppendorf tubes at 22 °C under aerobic conditions. The concentration of dG was 0.5 mM and the DNA-phosphate concentrations used were between 0.01 and 1.5 mM, corresponding to 0.0025–0.375 mM with regard to dG (assuming 25% of the bases are dG). The pH was controlled with Tris–HCl buffer (10 mM, pH 7.2) or phosphate buffer (0.5 or 50 mM, pH 7.2). Tris–HCl was also used for its hydroxyl radical scavenging properties [29], and in these experiments both dG and DNA concen-

Table 1
The absorbance (OD) of Fe^{3+} ($FeCl_3$, 0.1 mM) at concentrations of inorganic [PO_4^{3-}] or DNA-phosphate [DNA-P] between 0 and 1 mM, measured at 304 nm and 1 cm light path

Buffer type	Phosphate concentration-dependent increase in OD used for correction
Tris–HCl	$OD = 41.4 \times [PO_4^{3-}] + 0.264$
Tris–HCl	$OD = 19.0 \times [DNA\text{-}P] + 0.260$
Tris–maleate	$OD = 42.2 \times [PO_4^{3-}] + 0.289$
Tris–maleate	$OD = -3.7 \times [DNA\text{-}P] + 0.288$

OD was measured after 10 min. All buffers were 10 mM, pH 7.2. Values from five experiments ($n = 5$).

trations were 0.5 mM. Stock solutions of $FeSO_4$ were prepared in H_2SO_4 (0.25 mM) to prevent oxidation and an equimolar concentration of sodium hydroxide was added to each sample, to neutralise the H_2SO_4. The pH of samples without inorganic phosphate or Tris–HCl added were adjusted to approximately pH 7.2 with sodium hydroxide only (~ 0.5 mM, final concentration).

For samples containing dG in solution, HPLC analysis of 8-oxo-dG could be performed without further processing. Samples of DNA were transferred to Eppendorf vials and trichloroacetic acid (5% final concentration) to stop the reaction and to precipitate DNA. The precipitate (approximately 80 μg/sample) was then washed twice with 99.5% ethanol, air-dried for 15 min and finally dissolved in 100 μl of 20 mM sodium acetate buffer (pH 4.8). These samples were then stored frozen (− 30 °C) and analysis of 8-oxo-dG was done after enzymatic hydrolysis of DNA.

2.5. Enzymatic hydrolysis of DNA

To each DNA sample (80 μg), 20 μl of nuclease P1 (equivalent to 6 units, prepared in Tris–HCl buffer) was added and the samples were incubated at 37 °C for 30 min. Thereafter, 52 μl of alkaline phosphatase (equivalent to 1.3 DEA-units, prepared in Tris–HCl buffer) was added and the incubation continued at 37 °C for 60 min [11]. Hydrolysed samples were frozen (− 30 °C) until time for analysis.

2.6. HPLC analysis of 8-oxo-dG adduct and nucleosides

An HPLC equipped with a C18-reversed phase column (Hichrom, Kromasil-5μ, 150 × 4.6 mm) was used (flow: 1 ml/min) with an eluent composed of methanol (10 vol.%), citric acid (12.5 mM), sodium acetate (25 mM), NaOH (30 mM), and acetic acid (10 mM), pH 5.1 [11,30]. For detection of 8-oxo-dG, an electrochemical detector (BAS) with a glassy carbon electrode and an Ag/AgCl reference electrode was used (applied potential = 0.7 V) [30,31]. Intact nucleosides were analysed using an UV detector (254 nm) connected on line after the electrochemical detector.

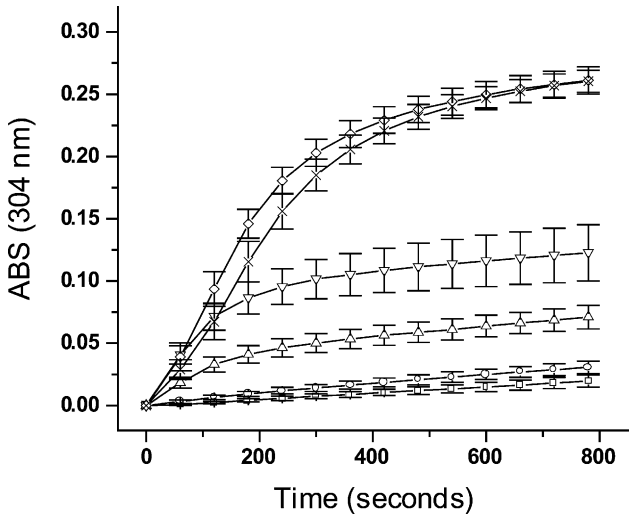

Fig. 2. The oxidation of Fe^{2+} ($FeSO_4$, 0.1 mM) in Tris–HCl buffer, 10 mM, pH 7.2, at different concentrations of calf thymus DNA-phosphate, 0–1 mM, measured at 304 nm. Symbols represent means and standard deviation from ten experiments. For clarity, only 1/3 of the measured data points (time interval) are presented in the figure. Concentrations of calf thymus DNA-phosphate: (□) 0 mM; (○) 0.01 mM; (△) 0.05 mM; (▽) 0.1 mM; (◇) 0.5 mM; and (×) 1 mM.

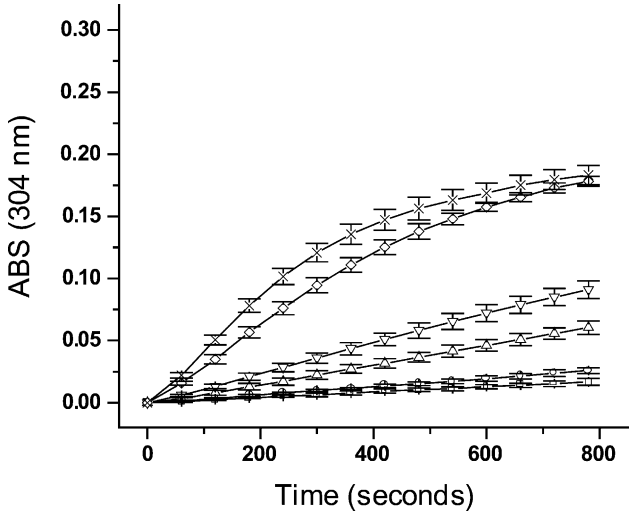

Fig. 1. The oxidation of Fe^{2+} ($FeSO_4$, 0.1 mM) in Tris–HCl buffer, 10 mM, pH 7.2, at different concentrations of inorganic phosphate, 0–1 mM, measured at 304 nm. Symbols represent means and standard deviation from six experiments. For clarity, only 1/3 of the measured data points (time interval) are presented in the figure. Concentrations of inorganic phosphate: (□) 0 mM; (○) 0.01 mM; (△) 0.05 mM; (▽) 0.1 mM; (◇) 0.5 mM; and (×) 1 mM.

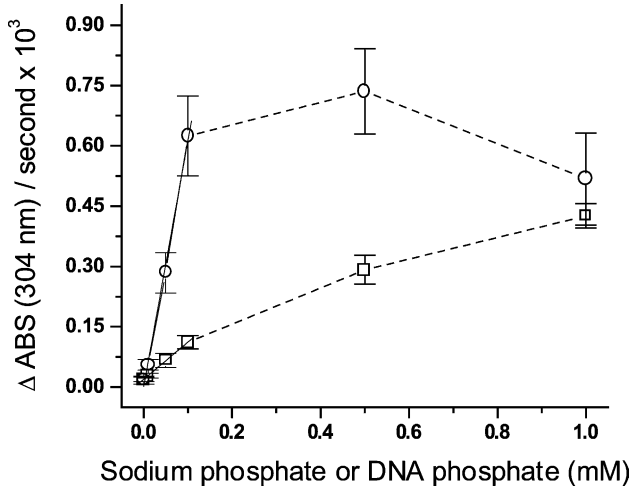

Fig. 3. Reaction rate for the oxidation of Fe^{2+} ($FeSO_4$, 0.1 mM) in Tris–HCl buffer, 10 mM, pH 7.2, at different concentrations of inorganic or calf thymus DNA-phosphate, 0–1 mM. Reaction rates are based on values from Figs. 1 and 2 for the linear increase of Fe^{2+} oxidation between 0 and 120 s. Symbols for inorganic phosphate represent means and standard deviation from six experiments. Symbols for calf thymus DNA-phosphate represent means and standard deviation from ten experiments. (□) Inorganic phosphate; (○) Calf thymus DNA-phosphate.

2.7. Calculation of results and statistic evaluation

To calculate the reaction rate for the formation of ferric ions, the initial (0–120 s) linear increase in absorbance at 304 nm was used, after correction for the change in absorption coefficient dependent on the concentration of inorganic phosphate, as described above. The HPLC chromatograms for 8-oxo-dG and dG were integrated with computer aid (ELDS, software from Chromatography Data Systems AB, Sweden) and quantified with external standards. The standard for dG was prepared from dG obtained from Fluka. The standard for 8-oxo-dG was prepared from 8-oxo-dG obtained from Sigma. The concentration of 8-oxo-dG was determined using a molar absorption coefficient of 12 300 M^{-1} cm^{-1} at 245 nm in H_2O [32]. The amount of 8-oxo-dG formed was presented as yield (nM) or as 8-oxo-dG formed per 10^5 dG molecules. To test for significant differences between mean values, the Student's *t*-test was used. Student's *t*-test was also used to test for significant differences between slopes of the regression lines in Figs. 3 and 5.

3. Results

3.1. Kinetics of Fe^{2+} oxidation at different concentrations of inorganic phosphate or DNA-phosphate

For both inorganic (Fig. 1) and DNA-phosphate (Fig. 2), increasing phosphate concentration correlated positively with an increased rate of oxidation of Fe^{2+} (0.1 mM). In inorganic phosphate, the rate of Fe^{2+} oxidation was clearly dependent on, and higher for every increase in the phosphate concentration used (0–1.0 mM), as can be seen in Fig. 1. The equation for the dependence of the initial (0–120 s) reaction rates ($Y = \Delta ABS/s$) on the inorganic phosphate concentration (X mM) for concentrations up to 0.1 mM, was $Y = 0.9 \times 10^{-3} \times X + 19 \times 10^{-6}$ ($r = 0.999$) (Fig. 3). The oxidation rate still increased with higher phosphate concentration (0.1–1.0 mM), but the increase was less pronounced (Fig. 3). This suggests that phosphate was the rate-limiting factor in the entire range (0–1.0 mM) of phosphate concentrations used (Fig. 3). For DNA-phosphate, up to a concentration of 0.1 mM, a linear correlation could also be seen initially (0–120 s) (Fig. 2). For DNA-phosphate, the

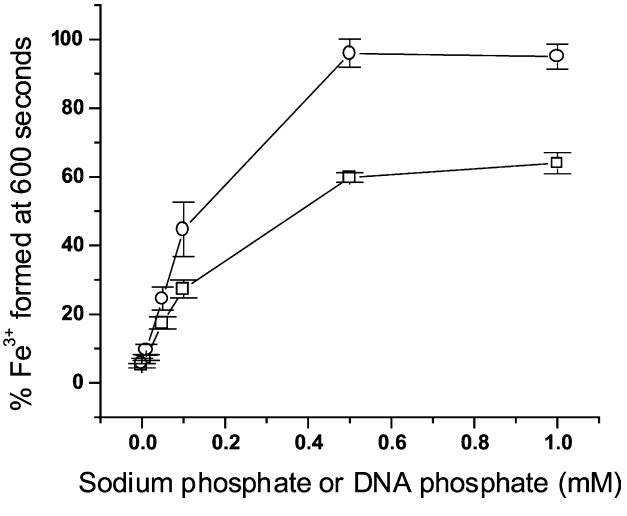

Fig. 4. Percent oxidation of Fe^{2+} ($FeSO_4$, 0.1 mM) to Fe^{3+} in Tris–HCl buffer, 10 mM, pH 7.2, at different concentrations of inorganic or calf thymus DNA-phosphate, 0–1 mM. Percent oxidised Fe^{2+} have been calculated from the absorbance values in Figs. 1 and 2 at time = 600 s. Symbols for inorganic phosphate represent means and standard deviation from six experiments. Symbols for calf thymus DNA-phosphate represent means and standard deviation from ten experiments. (□) Inorganic phosphate; (○) Calf thymus DNA-phosphate.

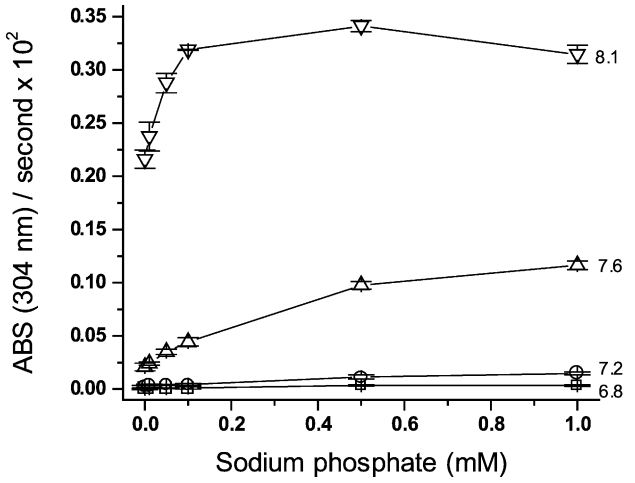

Fig. 5. Reaction rate for the oxidation of Fe^{2+} ($FeSO_4$, 0.1 mM) in Tris–maleate buffer, 10 mM, pH 6.8–8.1, at different concentrations of inorganic phosphate, 0–1 mM. Symbols represent values from four experiments. (□) pH 6.8; (○) pH 7.2; (△) pH 7.6; (▽) pH 8.1.

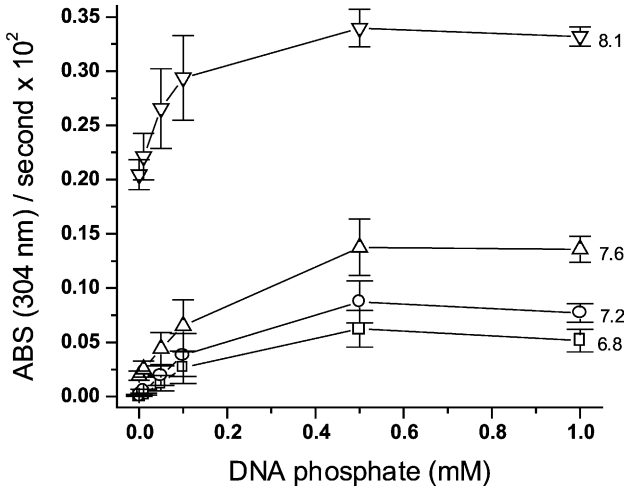

Fig. 6. Reaction rate for the oxidation of Fe^{2+} ($FeSO_4$, 0.1 mM) in Tris–maleate buffer, 10 mM, pH 6.8–8.1, at different concentrations of calf thymus DNA-phosphate, 0–1 mM. Symbols represent values from four experiments. (□) pH 6.8; (○) pH 7.2; (△) pH 7.6; (▽) pH 8.1.

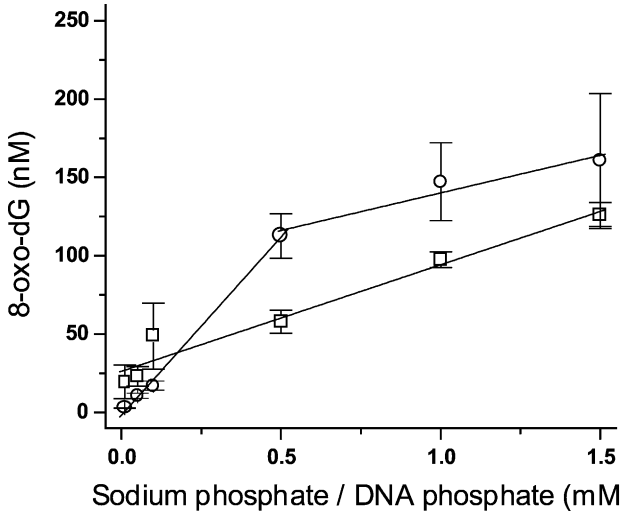

Fig. 7. Fe^{2+} ($FeSO_4$, 0.1 mM) catalyzed 8-oxo-dG formation (nM) in dG (0.5 mM) or calf thymus DNA (0.01–1.5 mM) in Tris–HCl buffer, 10 mM, pH 7.2 at different concentrations of inorganic phosphate or calf thymus DNA-phosphate, 0.01–1.5 mM. Reaction time is 10 min. All yields (nM) are presented as the increase over control (samples without iron). Symbols for dG and inorganic phosphate represent means and standard deviation from four experiments. Symbols for calf thymus DNA-phosphate represent means and standard deviation from six experiments. (□) dG and inorganic phosphate; (○) Calf thymus DNA-phosphate.

corresponding equation for the initial (0–120 s) rate of ferrous iron oxidation was $Y = 6.1 \times 10^{-3} \times X + 0.5 \times 10^{-6}$ ($r = 0.998$) for concentrations up to 0.1 mM, which is equimolar to the Fe^{2+} concentration used (Fig. 3). For DNA-phosphate concentrations above 0.1 mM (0.1–1.0 mM), the oxidation rate of Fe^{2+} was not influenced by DNA-phosphate concentration (Fig. 3).

3.2. Correlation between the yield of Fe^{3+} formation and concentrations of inorganic phosphate or DNA-phosphate

The rate of oxidation at different phosphate concentrations (Fig. 3) can also be recalculated to the yield of Fe^{3+} at a certain time. In Fig. 4, the [Fe^{3+}] at 600 s is presented in percent of 0.1 mM Fe^{3+} (100% oxidised). For inorganic and DNA-phosphate concentrations up to 0.1 mM, the yield of Fe^{3+} at this time point was linearly related to phosphate concentration ($R = 0.999$) (Fig. 4).

3.3. Effect of pH on the kinetics of Fe^{2+} oxidation in solutions of inorganic phosphate or DNA-phosphate

To further study variables that could influence the rate of oxidation of Fe^{2+} in these systems, the effect of pH on the reaction rates was followed with the use of Tris–maleate buffer as described in Materials and methods. Thus, as presented in Fig. 5, at pH 7.6, the rate increased several fold as compared to pH 6.8 and 7.2 while in solutions of DNA-phosphate, there was less influence by the increase of pH from 6.8 to 7.6 (Fig. 6). Also, as can be seen at pH 7.6, the difference in reaction rate for Fe^{2+} oxidation in inorganic phosphate and in solutions of DNA-phosphate observed at pH 7.2 were less pronounced. At pH 8.1, the effects of increased phosphate concentrations in the low range < 0.1 mM on the rate of oxidation was the highest for both inorganic and DNA-phosphate while at higher concentrations, the rate of Fe^{2+} oxidation was markedly less influenced (Figs. 5 and 6).

3.4. Fe^{2+}-mediated formation of 8-oxo-dG in dG and DNA at low phosphate concentrations

Under the same experimental conditions, the yield of 8-oxo-dG formed (Fig. 7) correlated positively with the phosphate concentration dependent yield of Fe^{3+} (Fig. 4). For DNA-phosphate (Fig. 7), the dG concentration necessarily varied with the phosphate concentration, and was thus 1/4 of respective phosphate concentration used (assuming 25% of bases to be dG). Due to the difference in dG concentration, the results in Fig. 7 were presented as the increase in concentration (nM) of 8-oxo-dG. The increase of 8-oxo-dG formation up to 1.5 mM of inorganic phosphate is

Table 2a
Modification by sodium phosphate buffer (PB) and scavenger (Tris–HCl) of the Fe^{2+}-induced formation of 8-oxo-dG in dG in solution

Modifier	Control	Fe^{2+} (0.1 mM)	Fe^{2+} (0.2 mM)
All solutions: dG (0.5 mM) and	8-oxo-dG/10^5 dG ± S.D.	Increase over control: 8-oxo-dG/10^5 dG ± S.D. (% 8-oxo-dG/10^5 dG ± S.D.)	Increase over control: 8-oxo-dG/10^5 dG ± S.D. (% 8-oxo-dG/10^5 dG ± S.D.)
(A) PB (50 mM)	1.5 ± 0.2	183 ± 5.7	324 ± 31
(B) PB (50 mM) and Tris–HCl (10 mM)	2.1 ± 1.0	74 ± 2.3 (60 ± 1.5)	131 ± 4.7 (59 ± 2.5)
(C) PB (0.5 mM)	1.5 ± 0.2	39 ± 3.5	56 ± 1.1
(D) PB (0.5 mM) and Tris–HCl (10 mM)	1.8 ± 0.5	12 ± 0.6 (69 ± 2.7)	16 ± 0.8 (71 ± 1.6)

Values represent observed yields from three independent experiments ($n = 3$).
Values in parenthesis reflect the percent decrease of 8-oxo-dG from the value in the row above.
Significance for column with Fe^{2+} (0.1 or 0.2 mM) in the difference between A and B (± Tris–HCl) or between C and D (± Tris–HCl) was $P < 0.001$ in all cases.
Reaction time is 10 min.

Table 2b
Modification by sodium phosphate buffer (PB) and scavenger (Tris–HCl) of the Fe^{2+}-induced formation of 8-oxo-dG in calf thymus DNA in solution

Modifier	Control	Fe^{2+} (0.1 mM)	Fe^{2+} (0.2 mM)
All solutions: DNA (0.5 mM) and	8-oxo-dG/10^5 dG ± S.D.	Increase over control: 8-oxo-dG/10^5 dG ± S.D. (% 8-oxo-dG/10^5 dG ± S.D.)	Increase over control: 8-oxo-dG/10^5 dG ± S.D. (% 8-oxo-dG/10^5 dG ± S.D.)
(A) PB (50 mM)	16 ± 6.9	61 ± 21	84 ± 19
(B) PB (50 mM) and Tris–HCl (10 mM)	13 ± 3.9	22 ± 11 (64 ± 8.4)	26 ± 7.1 (69 ± 1.8)
(C) No addition	14 ± 5.9	34 ± 8.4	55 ± 11
(D) Tris–HCl (10 mM)	17 ± 7.8	32 ± 8.0 (6.4 ± 35)	31 ± 9.2 (42 ± 18)

Values represent observed yields from four independent experiments ($n=4$).
Values in parenthesis reflect the percent decrease of 8-oxo-dG from the value in the row above.
Significance for column with Fe^{2+} (0.1 mM) in the difference between A and B (± Tris–HCl) was $0.01<P<0.05$, and for C and D (± Tris–HCl) $P>0.05$ (not significant). Significance for column with Fe^{2+} (0.2 mM) in the difference between A and B (± Tris–HCl) was $0.001<P<0.01$, and for C and D (± Tris–HCl) $0.01<P<0.05$.
Reaction time is 10 min.

linear ($R=0.979$); however, it cannot be excluded that there is a nick on the curve at 0.1 mM of phosphate (Fig. 7). For DNA-phosphate concentrations up to 0.5 mM, the linear ($R=0.999$) increase in the 8-oxo-dG formation was steeper than in the range 0.5–1.5 mM of DNA-phosphate (Fig. 7).

Under the same conditions as for Fig. 7, the relative increase of 8-oxo-dG (8-oxo-dG/10^5 dG) in solutions of inorganic phosphate or DNA-phosphate, in response to oxidation of 0.1 mM Fe^{2+} was 12 and 32 8-oxo-dG/10^5 dG, respectively (Tables 2a and 2b). Increasing the concentration of Fe^{2+} to 0.2 mM did not change the yield of 8-oxo-dG in the DNA system; however, in the absence of Tris–HCl, there was a significant increase of the yield in both systems (Tables 2a and 2b).

3.5. Fe^{2+}-mediated formation of 8-oxo-dG in dG and DNA at high phosphate concentrations

In high concentration (50 mM) of inorganic phosphate (with Tris–HCl added) and 0.1 mM Fe^{2+}, the relative yields of 8-oxo-dG were 73 and 22 for dG and DNA. These yields were significantly lower than those observed in the absence of Tris–HCl, e.g. 183 and 61, respectively (Tables 2a and 2b). Doubling the concentration of Fe^{2+} (0.2 mM) caused a significant increased formation of 8-oxo-dG in the absence of Tris–HCl for both inorganic phosphate and DNA-phosphate and only for inorganic phosphate when Tris–HCl was present.

3.6. Effect of scavenger and catalase on the Fe^{2+}-mediated formation of 8-oxo-dG in dG and DNA

The scavenging effect of Tris–HCl in all solutions of dG (Table 2a) was significant for all phosphate and Fe^{2+} concentrations used and in the range of 60–70%. In solutions of DNA (Table 2b), the only combination where the scavenging effect of Tris–HCl was not significant was in DNA-phosphate (0.5 mM) and Fe^{2+} (0.1 mM); here, the reduction in the yield of 8-oxo-dG was only 6.4%. With DNA-phosphate (0.5 mM) and Fe^{2+} (0.2 mM), the reduction was higher and significant, 42%. The highest reduction in yield, comparable to the system with free dG (Table 2a), was found with DNA in high concentration of phosphate buffer (50 mM), and for 0.1 and 0.2 mM Fe^{2+}, the reduction was 64% and 69%, respectively (Table 2b).

To verify the role of Fenton chemistry in systems with high phosphate concentrations, we studied the formation of 8-oxo-dG in the presence of catalase. In solutions of sodium phosphate buffer (50 mM, pH 7.2), after 10 min of reaction in presence of 0.01 mM Fe^{2+} and 5000 units/ml of catalase (equivalent to 120 μg protein/ml), the formation of 8-oxo-dG was inhibited by 94% in dG and by 93% in calf thymus DNA. The formation of 8-oxo-dG in dG was not influenced by the presence of heat-inactivated catalase (see Materials and methods), whereas in calf thymus DNA, the presence of heat-inactivated catalase reduced the formation of 8-oxo-dG around 50% (data not shown). Thus, in solutions of DNA, the relatively high concentration of catalase present may in part also act as a chemical scavenger.

4. Discussion

4.1. Phosphate-mediated oxidation of ferrous ions

We have previously reported that the yield of 8-oxo dG in gamma irradiated solutions of DNA was 20 times higher as compared to irradiated solutions of dG [26]. The radical chemistry in irradiated solutions of DNA or dG is complex, with a combination of indirect effects from radicals formed through radiolysis of water and effects from direct ionisations of the target molecules. To study whether the relatively high yields of 8-oxo-dG formed in irradiated solutions of DNA was unique for radiation-induced oxidative damage, solutions of dG and DNA were exposed to reactive oxygen species formed in Fenton type of reactions. Reactive oxygen

species were formed through oxidation of ferrous ions to ferric ions under aerobic conditions (Eqs. (1)–(4)). The rationale for the choice of this relatively simple system was that the rate of oxidation of Fe^{2+} could be followed as a function of the spectral change at 304 nm and controlled by the phosphate concentration (see Materials and methods).

Eqs. (1)–(3) describe the formation of reactive oxygen species in solutions of inorganic phosphate and ferrous ions. However, the dependence for chelation of Fe^{2+} to phosphate is not shown in the simplified equations, and as shown in the results, this is a rate-limiting step.

In Eq. (1B), the chelation of inorganic phosphate to Fe^{2+} is illustrated; however, the pK_a for $H_2PO_4^-$ and HPO_4^{2-} are 7.2 and 12, respectively; thus, at pH 7.2, the ratio between $[HPO_4^{2-}]/[H_2PO_4^-]$ is 1.0. As suggested from the results presented in Fig. 6, there is a pH effect on the rate of oxidation. For simplicity, reaction formulas without phosphate are presented.

$$Fe^{2+} + O_2 \leftrightarrow Fe^{3+} + O_2^-\cdot \quad (1)$$

$$(Fe^{2+}(H_2PO_4^-)_n)^{(2-n)} + O_2 \leftrightarrow (Fe^{3+}(H_2PO_4^-)_n)^{(3-n)} + O_2^-\cdot \quad (1B)$$

$$2O_2^-\cdot + 2H^+ \rightarrow H_2O_2 + O_2 \quad (2)$$

$$Fe^{2+} + H_2O_2 \rightarrow Fe^{3+} + \cdot OH + OH^- \quad (3)$$

$$Fe^{2+} + O_2 \rightarrow Fe^{2+} - O_2 \rightarrow Fe^{3+} + O_2^-\cdot \quad (4)$$

The oxidation of Fe^{2+} in complex with inorganic phosphate can be described by reaction Eq. (1) [10,33]. The superoxide ($O_2^-\cdot$) formed in reaction Eq. (1) can produce H_2O_2 in the dismutation reaction (Eq. (2)) [10,14,15,17,33]. The hydrogen peroxide-induced oxidation of ferrous ions will lead to the formation of hydroxyl radicals (Eq. (3)) [19,34]. Based on these reactions, for each •OH formed, a minimum of three Fe^{2+} will be oxidized. For DNA in solution, ferrous ions will bind to the phosphodiester leading to a localised production of hydroxyl radicals as supported by the findings of other researchers [21,24,25,35]. Eq. (4) illustrates the possible intermediate formation of a perferryl complex [17].

For DNA, results have been published that suggest that under aerobic conditions, DNA peroxyl radicals my react with ferrous iron (Eqs. (5)–(7)) [35,36].

$$DNA + \cdot OH \rightarrow DNA\cdot \quad (5)$$

$$DNA\cdot + O_2 \rightarrow DNAO_2\cdot \quad (6)$$

$$DNAO_2\cdot + Fe^{2+} + H^+ \rightarrow DNAO_2H + Fe^{3+} \quad (7)$$

The addition of phosphate ions has previously been shown to significantly enhance the rate of oxidation of Fe^{2+} [14,16,17], pointing out the dependence of inorganic- or DNA-phosphate concentration on the rate of oxidation. The rate of oxidation of Fe^{2+} correlated positively with the inorganic phosphate concentration within the range examined, 0–1 mM (Fig. 1), and for oxidation of Fe^{2+} in solutions of DNA-phosphate (Fig. 2) up to concentrations equimolar to Fe^{2+} (0.1 mM). However, the rate of oxidation of Fe^{2+} was seven times higher in the presence of DNA-phosphate up to 0.1 mM than in inorganic phosphate (Fig. 3). To explain the mechanism for this significant ($P < 0.001$) increase in the rate of Fe^{2+} oxidation by DNA-phosphate as compared to inorganic phosphate, more work is needed, and at this point, we can only verify the unique properties of the complex between DNA-phosphate and Fe^{2+}. A role of $DNAO_2$• in the oxidation process (Eq. (6)) is not a likely explanation to the high oxidation rate, as the yield of $DNAO_2$• would be expected to be low compared to available chelation sites on DNA-phosphate.

Under the experimental conditions used, the rate of ferrous ion oxidation was low until the complexing agents were added (Figs. 1 and 2) and as presented in Fig. 4, the absolute yield of Fe^{3+} formed during 10 min correlated with the inorganic- and DNA-phosphate concentrations. The correlation between the rate of oxidation and the DNA-phosphate concentration (Fig. 3) at equimolar concentrations of DNA-phosphate and Fe^{2+} (0.1 mM) provided optimal conditions, and no change in rate was seen in response to increased concentrations of DNA-phosphate. Thus, all DNA-phosphate groups (0.1–1.0 mM) are available as chelators for Fe^{2+}. As the rate of Fe^{2+} oxidation after about 300 s is not influenced by the DNA-phosphate concentration (0–0.1 mM) (Fig. 2), it may be suggested that the binding of Fe^{3+} for complexing sites on DNA-phosphate competes with the binding of Fe^{2+}, due to the high equilibrium constant (2.1×10^{14} M^{-1}) reported for the binding affinity of Fe^{3+} to DNA [37].

As expected, at a 5 to 10 times excess of DNA-phosphate, there was less competition for complexing sites of iron, and almost all the Fe^{2+} was oxidised within 600 s to yield Fe^{3+} (Figs. 2 and 4).

For inorganic phosphate, the positive correlation between oxidation rates and phosphate concentration up to 10 times excess of phosphate (highest tested) and the slower oxidation rate at excess concentrations of inorganic phosphate (Fig. 3), would suggest that the Fe^{2+} oxidation in inorganic phosphate is favoured in complexes with several phosphate molecules.

4.2. pH dependence for the rate of ferrous oxidation in solution of inorganic phosphate

At pH 7.2, the ratio between $[HPO_4^{2-}]/[H_2PO_4^-]$ is 1.0, and as shown in Fig. 5, increasing the pH to 7.6 in inorganic phosphate solution increased significantly the

rate of Fe^{2+} oxidation to the same rate as observed in solutions of DNA-phosphate. At this pH, the ratio between $[HPO_4^{2-}]/[H_2PO_4^-]$ has increased from 1.0 to 2.5, suggesting that the oxidation is favoured by formation of the Fe^{2+} complex with HPO_4^{2-}. The difference in catalytic activity may thus be explained by the degree of protonization of the two types of phosphates. This is supported by the increased binding constant of Fe^{2+} with HPO_4^{2-} (3981 M^{-1}) as compared to $H_2PO_4^-$ (501 M^{-1}) [38]. As expected, the pH effect observed for oxidation of Fe^{2+} in solutions of inorganic phosphate was not observed for DNA-phosphate mediated oxidation of Fe^{2+}, with a pK_a considerably lower than 7 for the DNA phosphodiester (Fig. 6). However, at pH 8.1, the phosphate-dependent oxidation rates of Fe^{2+} in both inorganic and DNA-phosphate (Figs. 5 and 6) were considerably increased only at the lowest phosphate concentrations. As shown in Fig. 6, there is also a pronounced spontaneous oxidation of Fe^{2+}; however, the possible interaction of the two processes has not been studied in detail here.

4.3. Formation of 8-oxo-dG in solutions of dG and DNA in presence of ferrous iron and phosphate

The formation of 8-oxo-dG in a solution of dG after addition of ferrous ions has been reported previously [30,39]. Floyd et al. [30] showed that in a solution of dG in bicarbonate buffer, the addition of ferrous ions alone, induced the formation of 8-oxo-dG. As the free radical scavengers thiourea and ethanol effectively inhibited the formation of 8-oxo-dG, while superoxide dismutase had very little effect, it may be suggested that the reaction was dependent on the formation of hydroxyl radicals. Analysis by spin-trapping technique revealed that the DNA–Fe^{2+} complex enhanced the formation of •OH from H_2O_2 [21]. These data support the mechanisms for phosphate-Fe^{2+} produced oxygen radical species as outlined in Eqs. (1)–(3).

The positive correlation between phosphate concentration and the yield of 8-oxo-dG is shown in Fig. 7 and relates to the phosphate-dependent increase in Fe^{2+} oxidation rate (Fig. 3). The formation of H_2O_2 from a Fenton-type reaction (Eqs. (1) and (3)) is the suggested mode of action in presence of high concentration of phosphate (50 mM) since the presence of catalase under these conditions efficiently inhibited the formation of 8-oxo-dG in experiments with either dG (94% inhibition) or calf-thymus DNA (93% inhibition) in solution (see Results). Heat-inactivated catalase did not inhibit the formation of 8-oxo-dG in solutions of dG. In DNA, however, around half of the inhibition of 8-oxo-dG formation in presence of catalase (see Results) could be due to chemical scavenging of radicals, possibly due to a protein–DNA interaction increasing the competition for the hydroxyl radicals formed. Further, in low phosphate concentrations (0.5 mM) the hydroxyl radical scavenger Tris–HCl decreased the yield of 8-oxo-dG in solutions of dG significantly (69–71%) (Results and Table 2a), supporting the primary role of hydroxyl radicals. For DNA-phosphate (0.5 mM), Tris–HCl decreased the yield of 8-oxo-dG to a lesser extent, only 6.4% with 0.1 mM Fe^{2+} and significantly (42%) with 0.2 mM Fe^{2+} (Results and Table 2b). The lower scavenging effect of Tris–HCl, seen in solutions of 0.5 mM DNA-phosphate without any inorganic phosphate present, may possibly be due to a localized production of hydroxyl radicals catalysed by the DNA-phosphate–Fe^{2+} complex as suggested in reactions (1)–(3). Under these conditions, the hydroxyl radicals would be formed close to, and reacting with DNA instead of Tris–HCl, this explaining the lesser efficiency of Tris–HCl to act as a radical scavenger. Formation of a perferryl complex as outlined in Eq. (4) would also be a possible explanation for the decreased efficiency of Tris–HCl. However, the role of •OH as the reactive species formed in the Fe^{2+} phosphate induced formation of 8-oxo-dG (and not metal oxygen complexes such as the ferryl ion, FeO^{2+}) is supported by electron spin resonance studies of the reaction of Fe^{2+} with H_2O_2 [40].

The addition of inorganic phosphate (50 mM) to DNA-phosphate (0.5 mM) increased the yield of 8-oxo-dG by 80% in 0.1 mM of Fe^{2+} while the corresponding increase was 50% in 0.2 mM Fe^{2+} (Table 2b). Assuming that the binding constant of Fe^{2+} to DNA-phosphate is in the range of that for Fe^{3+} (2.1×10^{14} M^{-1}), the orders of magnitude lower binding constants for $H_2PO_4^-$ and HPO_4^{2-} (501 and 3981 M^{-1}, respectively) would not be expected to change the localisation of production of oxygen reactive species, nor the types of oxygen species formed. However, the significant effect of radical scavengers (Tris–HCl) seen in the presence of 50 mM phosphate, and not in its absence (Table 2b), as well as the effect of catalase (see Results), seem to be contradictory to this assumption and rather indicate the formation of radicals outside the DNA-phosphate complex.

The marked increase of 8-oxo-dG in solutions of inorganic phosphate in response to 50 mM phosphate (Table 2a) is at least partly a consequence of that all the Fe^{2+} would be estimated to be oxidised under these conditions relative to the 60% in the presence of 0.5 mM phosphate (Fig. 4). However, since the increase in the yield of 8-oxo-dG in dG at high phosphate concentration (50 mM) is as much as five times higher as compared to low phosphate concentration (0.5 mM) (Table 2a), this would suggest that the oxidation is favoured by the complexing of each ferrous ion with several inorganic phosphate molecules, leading to an increased initial rate of H_2O_2 formation and hydroxyl radical production, and thus higher 8-oxo-dG formation.

4.4. Comparison of the effect of ferrous iron or radiation on the formation of 8-oxo-dG in solutions of dG and DNA

Recently published data for radiation induced formation of 8-oxo-dG showed that only a small fraction of the hydroxyl radicals formed through radiolysis of water will

lead to formation of 8-oxo-dG in solutions of dG [26]. The yield of hydroxyl radicals from radiolysis of water was 0.28 μmol J^{-1} [41], while the yield of 8-oxo-dG formed was 0.38×10^{-3} μmol J^{-1} [26]. Thus, only 0.14% of the •OH formed leads to the formation of 8-oxo-dG in solutions of dG. From the formulas given for the Fenton reaction (Eqs. (1)–(3)), the highest theoretical yield of •OH from 0.1 mmol Fe^{2+} would be 33 μmol, while the observed yield of 8-oxo-dG in 50 mM phosphate buffer was 0.92 μmol (recalculated from Table 2a), corresponding to 2.8% of the theoretical yield of •OH produced. The relative yield of 8-oxo-dG per unit •OH is thus around 20 times higher relative to the radiation-induced response. The lower yield of 8-oxo-dG in solutions of irradiated dG could be due to the formation of other end products than 8-oxo-dG, as the relative yield of 8-oxo-dG was only 0.3% of the total radiolysis of dG in comparison to 14.9% for DNA (see Table 1 in Ref. [26]). Thus, the reactive oxygen species formed through Fenton chemistry would favour the formation of 8-oxo-dG relative to the oxygen species formed in the process of radiolysis of water.

The radiation-induced formation of 8-oxo-dG from DNA was 7.7×10^{-3} μmol J^{-1} [26]; thus, 2.8% of the •OH formed led to the formation of 8-oxo-dG, a 20-fold higher yield as compared to irradiated dG in solution [26]. The observed yield of 8-oxo-dG in DNA-phosphate (0.5 mM) in response to oxidation of 0.1 mmol Fe^{2+} was 0.04 μmol (recalculated from Table 2b), corresponding to 0.12% of the •OH theoretically produced and 23 times lower than the corresponding yield in free dG. This can partly be explained by the presence of the other three bases competing for the reactive oxygen species. Based on the estimated yields of oxidative species (•OH), the relative yield of 8-oxo-dG in DNA from the Fenton reaction is several fold lower compared to the yield observed from irradiation.

To explain these observations, further experimental work is needed. Under conditions when hydroxyl radicals would be expected to be produced randomly and react by diffusion controlled mechanisms with the substrate, the dose–yield relationships would be expected to be similar for radiation and Fenton chemistry. The explanation for the higher yield of 8-oxo-dG in irradiated DNA versus the Fe^{2+} system could be due to electron transfer reactions taking place in the irradiated DNA favouring the formation of 8-oxo-dG [26].

5. Conclusions

The rate of ferrous ion oxidation under aerobic conditions correlated positively with the phosphate concentrations in solutions of inorganic or DNA-phosphate. Up to equimolar concentrations with regard to Fe^{2+}, the rate of oxidation was significantly higher in solutions of DNA-phosphate as compared to inorganic phosphate. The phosphate-mediated oxidation of ferrous ion leads to the formation of 8-oxo-dG in solutions of dG or DNA and the yield correlated positively with the yield of Fe^{3+} formed. The localised production of reactive oxygen species in solutions of DNA-phosphate was verified as addition of the radical scavenger Tris–HCl did not significantly decrease the yield of 8-oxo-dG.

The relative yields of 8-oxo-dG per unit Fe^{3+} formed were significantly higher in solutions of dG in inorganic phosphate as compared to DNA-phosphate solutions. Further studies are needed to explain the large differences in yields of 8-oxo-dG in the two model systems when exposed to Fenton chemistry relative to radiation induced radical reactions.

Acknowledgements

This work was supported by the Swedish Natural Science Research Council and the Swedish Radiation Protection Institute.

The authors are grateful for valuable discussions with professor Lars Ehrenberg and Dr. Siv Osterman-Golkar during the progress of this work.

References

[1] B. Halliwell, O.I. Aruoma, DNA damage by oxygen-derived species—its mechanism and measurement in mammalian systems, FEBS Lett. 281 (1991) 9–19.
[2] M.G. Simic, D.S. Bergtold, L.R. Karam, Generation of oxy radicals in biosystems, Mutat. Res. 214 (1989) 3–12.
[3] B.N. Ames, Endogenous DNA damage as related to cancer and aging, Mutat. Res. 214 (1989) 41.
[4] B.N. Ames, Mutagenesis and carcinogenesis: endogenous factors and axogenous factors, Environ. Mol. Mutagen. 14 (1989) 66.
[5] M. Hayakawa, K. Torii, S. Sugiyama, M. Tanaka, T. Ozawa, Age-associated accumulation of 8-hydroxydeoxyguanosine in mitochondrial DNA of human diaphragm, Biochem. Biophys. Res. Commun. 179 (1991) 1023.
[6] S. Loft, K. Vistisen, M. Ewertz, A. Tjönneland, K. Overvad, H. Enghusen Poulsen, Oxidative DNA damage estimated by 8-hydroxydeoxyguanosine excretion in humans: influence of smoking, gender and body mass, Carcinogenesis 13 (1992) 2241.
[7] A.P. Grollman, M. Moriya, Mutagenesis by 8-oxoguanine—an enemy within, Trends Genet. 9 (1993) 246–249.
[8] B. Halliwell, J.M.C. Gutteridge, Oxygen toxicity, oxygen radicals, transition metals and disease, Review articleBiochem. J. 219 (1984) 1–14.
[9] M.L. Michaels, J.H. Miller, The GO system protects organisms from the mutagenic effect of the spontaneous lesion 8-hydroxyguanine (7,8-dihydro-8-oxoguanine), J. Bacteriol. 174 (1992) 6321–6325.
[10] G. Minotti, S.D. Aust, An investigation into the mechanism of citrate-Fe^{2+}-dependent lipid peroxidation, Free Radic. Biol. Med. 3 (1987) 379–387.
[11] H. Kasai, P.F. Crain, Y. Kuchino, S. Nishimura, A. Ootsuyama, H. Tanooka, Formation of 8-hydroxyguanine moiety in cellular DNA by agents producing oxygen radicals and evidence for its repair, Carcinogenesis 7 (1986) 1849–1851.
[12] K. Sakumi, M. Sekiguchi, Structures and functions of DNA glycosylases, Mutat. Res. 236 (1990) 161–172.
[13] J.Y. Mo, H. Maki, M. Sekiguchi, Hydrolytic elimination of a mutagenic nucleotide, 8-oxodGTP, by human 18-kilodalton protein-sani-

tization of nucleotide pool, Proc. Natl. Acad. Sci. U.S.A. 89 (1992) 11021–11025.
[14] D.M. Miller, G.R. Buettner, S.D. Aust, Transition metals as catalysts of "autoxidation" reactions, Free Radic. Biol. Med. 8 (1990) 95–108.
[15] H.B. Dunford, Free radicals in iron-containing systems, Free Radic. Biol. Med. 3 (1987) 405–421.
[16] M. Cher, N. Davidson, The kinetics of the oxygenation of ferrous iron in phosphoric acid solution, J. Am. Chem. Soc. 77 (1955) 793–798.
[17] J.M. Gutteridge, Hydroxyl radical formation from the auto-reduction of a ferric citrate complex, Free Radic. Biol. Med. 11 (1991) 401–406.
[18] D.C. Harris, P. Aisen, Facilitation of Fe(II) autoxidation by Fe(III) complexing agents, Biochim. Biophys. Acta 329 (1973) 156–158.
[19] J.D. Rush, Z. Maskos, W.H. Koppenol, Reactions of iron(II) nucleotide complexes with hydrogen peroxide, FEBS Lett. 261 (1990) 121–123.
[20] J.E. Biaglow, A.V. Kachur, The generation of hydroxyl radicals in the reaction of molecular oxygen with polyphosphate complexes of ferrous ion, Radiat. Res. 148 (1997) 181–187.
[21] R.A. Floyd, DNA-ferrous iron catalyzed hydroxyl free radical formation from hydrogen peroxide, Biochem. Biophys. Res. Commun. 99 (1981) 1209–1215.
[22] R.A. Floyd, Direct demonstration that ferrous ion complexes of di- and triphosphate nucleotides catalyze hydroxyl radical formation from hydrogen peroxide, Arch. Biochem. Biophys. 225 (1983) 263–270.
[23] A.V. Kachur, Y. Manevich, J.E. Biaglow, Effect of purine nucleoside phosphates on OH-radical generation by reaction of Fe^{2+} with oxygen, Free Radic. Res. 26 (1997) 399–408.
[24] W.F. Blakely, A.F. Fuciarelli, B.J. Wegher, M. Dizdaroglu, Hydrogen peroxide-induced base damage in deoxyribonucleic acid, Radiat. Res. 121 (1990) 338–343.
[25] E.S. Henle, Y. Luo, W. Gassmann, S. Linn, Oxidative damage to DNA constituents by iron-mediated Fenton reactions: the deoxyguanosine family, J. Biol. Chem. 271 (1996) 21177–21186.
[26] P. Svoboda, M. Harms-Ringdahl, Protection or sensitisation by thiols or ascorbate in irradiated solutions of DNA or deoxyguanosine, Radiat. Res. 151 (1999) 605–616.
[27] J.D. Rush, W.H. Koppenol, Reactions of Fe(II)–ATP and Fe(II)–citrate complexes with *t*-butyl hydroperoxide and cumyl hydroperoxide, [published erratum appears in FEBS Lett. 280 (2) (1991 Mar 25) 400], FEBS Lett. 275 (1990) 114–116.
[28] N.E. Good, G.D. Winget, W. Winter, T.N. Connolly, S. Izawa, R.M.M. Singh, Hydrogen ion buffers for biological research, Biochemistry 5 (1966) 467–477.
[29] M. Hicks, J.M. Gebicki, Rate constants for reaction of hydroxyl radicals with Tris–HCl: Tricine and Hepes buffers, FEBS Lett. 199 (1986) 92–94.
[30] A. Floyd, J.J. Watson, P.K. Wong, D.H. Altmiller, R.C. Rickard, Hydroxyl free radical adduct of deoxyguanosine: sensitive detection and mechanisms of formation, Free Radic. Res. Commun. 1 (1986) 163–172.
[31] J.W. Park, K.C. Cundy, B.N. Ames, Detection of DNA adducts by high-performance liquid chromatography with electrochemical detection, Carcinogenesis 10 (1989) 827–832.
[32] H. Kasai, S. Nishimura, Hydroxylation of deoxyguanosine at C-8 position by ascorbic acid and other reducing agents, Nucleic Acids Res. 12 (1984) 2137–2145.
[33] M.L. Muiras, P.U. Giacomoni, P. Tachon, Modulation of DNA breakage induced via the Fenton reaction, Mutat. Res. 295 (1993) 47–54.
[34] I. Yamazaki, L.H. Piette, ESR spin-trapping studies on the reaction of Fe^{2+} ions with H_2O_2-reactive species in oxygen toxicity in biology, J. Biol. Chem. 265 (1990) 13589–13594.
[35] E.S. Henle, S. Linn, Formation, prevention, and repair of DNA damage by iron/hydrogen peroxide, Minireview. J. Biol. Chem. 272 (1997) 19095–19098.
[36] E.S. Henle, Y. Luo, S. Linn, Fe^{2+}, Fe^{3+}, and oxygen react with DNA-derived radicals formed during iron-mediated Fenton reactions, Biochemistry 35 (1996) 12212–12219.
[37] L.E. Netto, A.M. Ferreira, O. Augusto, Iron(III) binding in DNA solutions: complex formation and catalytic activity in the oxidation of hydrazine derivatives, Chem. Biol. Interact. 79 (1991) 1–14.
[38] A.E. Martell, R.M. Smith, in: Critical Stability Constants, vol. 5, Plenum, New York, 1988, first supplement.
[39] N. Murata-Kamiya, H. Kamiya, M. Muraoka, H. Kaji, H. Kasai, Comparison of oxidation products from DNA components by gamma-irradiation and Fenton-type reactions, J. Radiat. Res. 38 (1997) 121–131.
[40] S. Croft, B.C. Gilbert, J.R.L. Smith, A.C. Whitwood, An ESR investigation of the reactive intermediate generated in the reaction between FeII and H_2O_2 in aqueous solution-direct evidence for the formation of the hydroxyl radical, Free Radic. Res. Commun. 17 (1992) 21–39.
[41] C. von Sonntag, The Chemical Basis of Radiation Biology, Taylor & Francis, London, 1987.